Possible phase diagram for localization tuned by the disorder and Pauli-blocking effects

A. Kwang-Hua Chu*
Department of Physics, Northwest Normal University, Gansu, Lanzhou 730070, People's Republic of China
(Received 8 July 2003; published 17 November 2003)

Based on the acoustic analog, we investigate both of the effects, disorder and (Pauli-blocking) interaction, on the possible localization in electron gases by using the quantum discrete kinetic model. We present effects of the disorder (or free orientation θ which is related to the relative direction of scattering of particles with respect to the normal of the propagating plane-wave front) which is introduced into the Ühling-Uhlenbeck equations together with those of the Pauli-blocking. We obtain a possible phase diagram (related to the strength of disorders and the mean free path) which qualitatively resembles that proposed by Abrahams [Ann. Phys. (Leipzig) **8**, 539 (1999)].

DOI: 10.1103/PhysRevB.68.205308 PACS number(s): 71.10.Hf, 71.30.+h, 73.20.Jc, 73.20.Fz

I. INTRODUCTION

Recently some developments in the localization problem[1] have become a major theme in the condensed matter research. One example is the strongly interacting electron (non-Fermi) liquid with different strengths of disorder.[2] Interesting issues are the quantum phase transition and quantum critical point, etc., as reviewed in Ref. 2. Both effects of disorder and interaction are closely relevant to the weak and strong localization.[3,4] They are then related to the metal-insulator transition in two dimensions. Although most of theories proposed before are based on the Fermi liquid behavior, new insights could be obtained considering the possible analogy with superconducting transition which might be related to the bosonic system.[5]

Note that studies of classical wave mechanical systems have some important advantages over quantum mechanical wave systems even there are similarities in between. In a mesoscopic system, where the sample size is smaller than the mean free path for an elastic scattering, it is satisfactory for a one-electron model to solve the time-independent Schrödinger equation

$$-\frac{\hbar^2}{2m}\nabla^2\psi+V'(\vec{r})\psi=E\psi,$$

or (after dividing by $-\hbar^2/2m$)

$$\nabla^2\psi+[q^2-V(\vec{r})]\psi=0, \tag{1}$$

where q is an (energy) eigenvalue parameter, which for the quantum-mechanic system is $\sqrt{2mE/\hbar^2}$.

Meanwhile, the equation for classical (scalar) waves is

$$\nabla^2\psi-\frac{1}{c^2}\frac{\partial^2\psi}{\partial t^2}=0$$

or (after applying a Fourier transform in time and contriving a system where c (the wave speed) varies with position $\vec{r}$)

$$\nabla^2\psi+[q^2-V(\vec{r})]\psi=0; \tag{2}$$

here the eigenvalue parameter q is ω/c_0, where ω is a natural (or an eigen) frequency and c_0 is a reference wave speed. Comparing the time dependencies one gets the quantum and classical relation $E=\hbar\omega$.

It seems that the control and observability of the classical experimental analogs may be matched by analytical works or numerical simulations. However, classical systems could be used to study time-dependent potential fields and nonlinear effects, which are very difficult and time consuming to treat numerically or analytically. Motivated by the analogy between electrons in periodic or disordered metals and waves in classical acoustical systems, an investigation for observing classical (Anderson) localization[3] using the quantum discrete kinetic model was performed, and will be presented here.

Plane (sound) wave propagation in dilute monatomic (hard-sphere) gases has been successfully investigated by continuous and/or discrete kinetic models since the 1960s (Refs. 6 and 7) (please see the detailed cited references therein). Relevant initial and/or boundary value problems—i.e., the former being central to the analytical or numerical approach because of the propagation of the forced sound from a certain origin, and the latter being almost related to the experimental environment due to the sensors and transducers located somewhere downstream—must be well defined and then solved to obtain the complex spectra or dispersion relations (real part: sound dispersion; imaginary part: sound attenuation or absorption). In comparison with experiments, results of the continuous velocity approach gave a better fit than the discrete velocity approach. The integral form of the former,[6] however, may smooth out some peculiar phenomena or only give a *bulk* physical behavior considering the continuous distribution of the particle velocities. The discrete form of the latter, i.e., particle velocities (and the associated number density) being a finite set while keeping the space and time continuous, provides us possibilities to adjust the discrete velocity, e.g., the free orientation of it in the two-dimensional (2D) plane (which could be thought as a kind of disorder for coplanar velocity models) and solve relevant problems in order to gain more physical insights for specific interests. For instance, a molecular beam interacting with surfaces (solids or liquids) will normally depend on some specific incident or reflecting angles. Wave propagation in random or disordered media might be another case.[8–10]

 ©2003 The American Physical Society

Both theories and measurements are in rapid progress, for the latter, acoustical analogs considering continuum-mechanical and quantum-mechanical approaches are included.[11]

As a continuous attempt,[7] adopting the quantum analog of the discrete kinetic model and the Uhling-Uhlenbeck collision term, which could describe the collision of a gas of dilute hard-sphere Fermi or Bose particle by tuning a parameter γ [via a *Pauli blocking factor* of the form $1+\gamma f$ with f being a normalized (continuous) distribution function giving the number of particles per cell, say, a unit cell, in phase space], in this paper we plan to investigate the possible static[12] and/or dynamic localization which relates to the dispersion relations of plane waves propagating in electron gases by introducing a disorder or free orientation (θ which is related to the relative direction of scattering of particles with respect to the normal of the propagating plane-wave front[13–16]) into the quantum discrete kinetic model (which has been verified in Refs. 7 and 13–15). This presentation will give us more clues for the studies of the quantum wave dynamics in 2D electron gases and the possible appearance of a localization which is directly linked to the particles (number) density and their energy states.

In the following presentation, based on the acoustical analogs (considering the continuum-mechanical and quantum-mechanical approaches in between[11,15]), we shall demonstrate the possible phase diagram related to the route to the quantum critical point proposed by Abrahams.[1] Note that our previous results,[15–17] in which θ is a disorder parameter, indicate that for $\theta=0$ (larger disorder) and $\theta=\pi/4$ (smaller disorder), there exist gaps of spectra and possible (dynamical) localization which are similar to those reported in Refs. 9–12. Our (quantum kinetic) approach, as it includes the nonuniform variation of those transport coefficients, such as viscosity and thermal conductivity, which are directly linked to the mean free path of the gas,[7] will thus give researchers more insights for similar problems, especially for the current interest in interacting 2D electron gases.

II. FORMULATIONS

We assume that the gas is composed of identical hard-sphere particles of the same mass.[7,13,14] The velocities of these particles are restricted to, e.g.,: $\mathbf{u}_1,\mathbf{u}_2,\cdots,\mathbf{u}_p$; p is a finite positive integer. The discrete number densities of particles are denoted by $N_i(\mathbf{x},t)$ associated with the velocities $\mathbf{u}_i$ at point $\mathbf{x}$ and time t. If only nonlinear binary collisions and the evolution of N_i are considered, we have

$$\frac{\partial N_i}{\partial t}+\mathbf{u}_i\cdot\nabla N_i=F_i\equiv\sum_{j=1}^{p}\sum_{(k,l)}(A_{kl}^{ij}N_kN_l-A_{ij}^{kl}N_iN_j),$$

$$i=1,\cdots,p, \tag{3}$$

where (k,l) are admissible sets of collisions.[7,13–17] We may also define the right-hand side of the above equation as

$$F_i(N)=\frac{1}{2}\sum_{j,k,l}(A_{kl}^{ij}N_kN_l-A_{ij}^{kl}N_iN_j), \tag{4}$$

with $i\in\Lambda=\{1,\cdots,p\}$. Here, the summation is taken over all $j,k,l\in\Lambda$, where A_{kl}^{ij} are non-negative constants satisfying[7,13,14] $A_{kl}^{ji}=A_{kl}^{ij}=A_{lk}^{ij}$, the indistinguishability of the particles in collision; $A_{kl}^{ij}(\mathbf{u}_i+\mathbf{u}_j-\mathbf{u}_k-\mathbf{u}_l)=0$, the conservation of momentum in the collision; and $A_{kl}^{ij}=A_{ij}^{kl}$, the microreversibility condition. The conditions defined for the discrete velocities above require that there are elastic, binary collisions, such that the momentum and energy are preserved, i.e., $\mathbf{u}_i+\mathbf{u}_j=\mathbf{u}_k+\mathbf{u}_l$ and $|\mathbf{u}_i|^2+|\mathbf{u}_j|^2=|\mathbf{u}_k|^2+|\mathbf{u}_l|^2$ are possible for $1\leqslant i,j,k,l\leqslant p$.

The collision operator is now simply obtained by joining A_{ij}^{kl} to the corresponding transition probability densities a_{ij}^{kl} through $A_{ij}^{kl}=S|\mathbf{u}_i-\mathbf{u}_j|a_{ij}^{kl}$, where

$$a_{ij}^{kl}\geqslant 0,\quad \sum_{k,l=1}^{p}a_{ij}^{kl}=1,\quad \forall i,j=1,\cdots,p;$$

with S being the effective collisional cross section.[7,13–17] If all $n(p=2n)$ outputs are assumed to be equally probable, then $a_{ij}^{kl}=1/n$ for all k and l; otherwise $a_{ij}^{kl}=0$.

The term $S|\mathbf{u}_i-\mathbf{u}_j|dt$ is the volume spanned by the particle with $\mathbf{u}_i$ in the relative motion with respect to the molecule with $\mathbf{u}_j$ in the time interval dt. Therefore, $S|\mathbf{u}_i-\mathbf{u}_j|N_j$ is the number of j particles involved by the collision in unit time. Collisions satisfying the conservation and reversibility conditions which have been stated above are defined as *admissible collisions*.[7,15–17]

The simplified discrete kinetic model, i.e., the $2\times n$ velocity model,[7,14–17] is to consider a one-component discrete velocity gas such that the particles can attain $2n$ velocities in the 2D plane. In particular, the velocity discretization is characterized by (i) $|\mathbf{u}_i|=c$, (ii) $\mathbf{u}_i+\mathbf{u}_{i+n}=0$, and (iii) $\mathbf{u}_i\cdot\mathbf{u}_{i+1}=c^2\cos(\pi/n)$, $i=1,\ldots,2n$, where the index is to be intended modulo $2n$, i.e., $i\equiv i+2n$. Such a model is called the planar $2n$ velocity model. If only elastic collisions are taken into account, then the nontrivial admissible ones (where this term is used to denote those collisions which produce nonvanishing terms in the collision operator) are

$$\text{head-on encounters:}\quad (\mathbf{u}_i,\mathbf{u}_{i+n})\leftrightarrow(\mathbf{u}_j,\mathbf{u}_{j+n}),$$

$$\forall j\neq i, i=1,\ldots,2n.$$

Meanwhile, the momentum and energy are presumably preserved:

$$\mathbf{u}_i+\mathbf{u}_{i+n}=\mathbf{u}_j+\mathbf{u}_{j+n},\quad |\mathbf{u}_i|^2+|\mathbf{u}_{i+n}|^2=|\mathbf{u}_j|^2+|\mathbf{u}_{j+n}|^2.$$

Moreover, all the velocity directions after collisions are assumed to be equally probable. For example, there are admissible collisions $(\mathbf{u}_1,\mathbf{u}_3)\leftrightarrow(\mathbf{u}_2,\mathbf{v}_u)$ as $n=2$.[7,14–17] We note that the summation of $N_i(\Sigma_iN_i)$, the total discrete number density here, is related to the macroscopic density ρ $(=m_p\Sigma_iN_i)$, where m_p is the mass of the particle.[13–16]

Together with the introduction of the Uhling-Uhlenbeck collision term[7,13]

$$F_i=\sum_{j,k,l} A_{kl}^{ij}[N_kN_l(1+\gamma N_i)(1+\gamma N_j) - N_iN_j(1+\gamma N_k)(1+\gamma N_l)], \tag{5}$$

into Eq. (3) or (4), for $\gamma<0$ (normally, $\gamma=-1$), we can then obtain a quantum discrete kinetic equation for a gas of Fermi particles; while for $\gamma>0$ (normally, $\gamma=1$) we obtain one for a gas of Bose particles, and for $\gamma=0$ we recover Eq. (3). Considering binary collisions only, from Eq. (5) the model of the quantum discrete Boltzmann equation for Fermi or Bose gases proposed in Refs. 7 and 13 is then a system of $2n$ $(=p)$ semilinear partial differential equations of the hyperbolic type:

$$\frac{\partial}{\partial t}N_i+\mathbf{v}_i\cdot\frac{\partial}{\partial \mathbf{x}}N_i =\frac{cS}{n}\sum_{j=1}^{2n} N_jN_{j+n}(1+\gamma N_{j+1})(1+\gamma N_{j+n+1}) -2cSN_iN_{i+n}(1+\gamma N_{i+1})(1+\gamma N_{i+n+1}),$$

$$i=1,\ldots,2n, \tag{6}$$

where $N_i=N_{i+2n}$ are unknown functions, and $\mathbf{v}_i=c(\cos[\theta+(i-1)\pi/n],\sin[\theta+(i-1)\pi/n])$; c is a reference velocity modulus and the same order of magnitude as that (c is the sound speed in the absence of scatters) used in Ref. 9, θ is the orientation starting from the positive x axis to the u_1 direction and could be thought of as a parameter for introducing a *disorder*,[10–12,15–17] and S is an effective collision cross section for the collision system.

Since passage of the sound wave will cause a small departure from an equilibrium state and result in energy loss owing to internal friction and heat conduction, we linearize the above equations around a uniform equilibrium state (the particles number density is N_0) by setting $N_i(t,x)=N_0[1+P_i(t,x)]$, where P_i is a small perturbation. The equilibrium state here is presumed to be the same as in Refs. 7, 13, and 16. First, we have (say, $i=m$)

$$\frac{\partial}{\partial t}P_m+\mathbf{v}_m\cdot\frac{\partial}{\partial \mathbf{x}}P_m+2cSN_0[(P_m+P_{m+n}) +\gamma N_0(P_m+P_{m+n}+P_\Sigma)+\cdots] =\frac{cSN_0}{n}\sum_{k=1}^{2n}[(P_k+P_{k+n}+\gamma N_0 \times(P_k+P_{k+n}+P_{sum})+\cdots]; \tag{7}$$

here, $m=1,\ldots,2n$, $P_{sum}=0$ for $n=2$ because of the restriction for the total perturbations in an equilibrium state and the remaining terms in both sides are higher order terms related to $(\gamma N_0)^2$. The linearized version of the above equation is

$$\frac{\partial}{\partial t}P_m+\mathbf{v}_m\cdot\frac{\partial}{\partial \mathbf{x}}P_m+2cSN_0(P_m+P_{m+n})(1+\gamma N_0) =\frac{2cSN_0}{n}\sum_{k=1}^{2n}P_k(1+\gamma N_0). \tag{8}$$

In these equations after replacing the index m with $m+n$, and using the identities $P_{m+2n}=P_m$, we then have

$$\frac{\partial}{\partial t}P_{m+n}-\mathbf{v}_m\cdot\frac{\partial}{\partial \mathbf{x}}P_{m+n}+2cSN_0(P_m+P_{m+n})(1+\gamma N_0) =\frac{2cSN_0}{n}\sum_{k=1}^{2n}P_k(1+\gamma N_0). \tag{9}$$

Combining the above two equations, first adding then subtracting, with $A_m=(P_m+P_{m+n})/2$ and $B_m=(P_m-P_{m+n})/2$, we can have

$$\frac{\partial}{\partial t}A_m-c\cos\left[\theta+\frac{(m-1)\pi}{n}\right]\frac{\partial}{\partial x}B_m+4cSN_0A_m(1+\gamma N_0) =\frac{4cSN_0}{n}\sum_{k=1}^{2n}A_k(1+\gamma N_0), \tag{10}$$

$$\frac{\partial}{\partial t}B_m+c\cos\left[\theta+\frac{(m-1)\pi}{n}\right]\frac{\partial}{\partial x}A_m=0,\quad m=1,\ldots,2n. \tag{11}$$

Note that $\partial P_m/\partial y=0$, as P_m only varies along the wave propagating direction: the x-axis direction. From $P_{m+2n}=P_m$, and with $A_m=(P_m+P_{m+n})/2$ and $B_m=(P_m-P_{m+n})/2$, we can have $A_{m+n}=A_m$, $B_{m+n}=-B_m$.

After some similar manipulations, as mentioned in Refs. 7 and 16, with $B=\gamma N_0<0$,[7,13] which gives or defines the (proportional) contribution from the Fermi gases (if $\gamma<0$, e.g., $\gamma=-1$), we then have

$$\left\{\frac{\partial^2}{\partial t^2}+c^2\cos^2\left[\theta+\frac{(m-1)\pi}{n}\right]\frac{\partial^2}{\partial x^2}+4cSN_0(1+B)\frac{\partial}{\partial t}\right\}D_m =\frac{4cSN_0(1+B)}{n}\sum_{k=1}^{n}\frac{\partial}{\partial t}D_k, \tag{12}$$

where $D_m=(P_m+P_{m+n})/2$, $m=1,\cdots,n$, since $D_1=D_m$ for $1=m \pmod{2n}$.

We are ready to look for the solutions in the form of plane wave $D_m=a_m\exp i(kx-\omega t)$, $(m=1,\ldots,n)$, with $\omega=\omega(k)$. This is related to the dispersion relations of 1D (forced) plane wave propagation in Fermi gases. So we have

$$\left(1+ih(1+B)-2\lambda^2\cos^2\left[\theta+\frac{(m-1)\pi}{n}\right]\right)a_m -\frac{ih(1+B)}{n}\sum_{k=1}^{n}a_k=0,\quad m=1,\cdots,n, \tag{13}$$

where

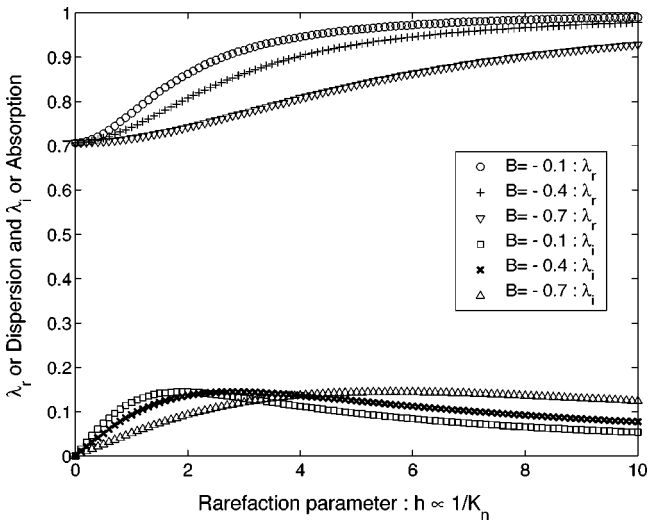

FIG. 1. Variations of λ_r and λ_i with respect to h for different B's (away from $B=-1$) $B=\gamma N_0$, γ corresponds to -1; λ_r denotes the dispersion and λ_i denotes the attenuation. $h=4cSN_0/\omega$, S is the effective collision cross-section.

$$\lambda = kc/(\sqrt{2}\omega), h(1+B) = h_b = 4cSN_0(1+B)/\omega \quad \propto 1/K_n,$$

$h_b = h(1+B)$ or h is the rarefaction parameter of the gas, whereas, for $B=0$, h is the rarefaction parameter of the Boltzmann-particle gas;[7] K_n is the Knudsen number which is defined as the ratio of the mean free path of gases to the wave length of the plane (sound) wave.

Let $a_m = \mathcal{C}/(1+ih_b - 2\lambda^2\cos^2[\theta+(m-1)\pi/n])$, where $\mathcal{C}$ is an arbitrary, unknown constant, since we here only have interest in the eigenvalues of above relation. The eigenvalue problems for different $2\times n$ velocity models reduces to

$$1 - \frac{ih_b}{n}\sum_{m=1}^{n} \frac{1}{1+ih_b - 2\lambda^2\cos^2\left[\theta + \dfrac{(m-1)\pi}{n}\right]} = 0. \tag{14}$$

III. RESULTS AND DISCUSSIONS

We can obtain the complex roots ($\lambda = \lambda_r + i\lambda_i$) from the polynomial equation above by using the standard mathematical (symbolic) or numerical software, e.g., MATHEMATICA or MATLAB.[7] The roots are the values for the nondimensionalized dispersion (positive real part, and a relative measure of the sound or phase speed) and the attenuation or absorption (positive imaginary part), respectively. B could be related to the occupation number of different-statistic particles of gases as we noticed the similarity in between from Ref. 7. We plot the main results in Figs. 1, 2, 3, 4, 5, and 6, respectively. We shall review the general characteristic dispersion relations for dilute atomic gases as reported in Ref. 7 before we interpret our present results for electron gases and/or non-Fermi gases.

Both families of curves in Fig. 1 (for $h \geqslant 0$) follow the conventional dispersion relations of plane waves propagating in dilute Bose and Boltzmann gases.[6,7] Our results show that once $|B|$ increases, the dispersion (λ_r) will reach the hydrodynamical limit ($h\to\infty$) rather slowly. Meanwhile, the maximum absorption (or attenuation) for all the rarefaction parameters h keeps the same for all B as observed in the lower part of Fig. 1. There are only shifts of the maximum absorption state (defined as h_{max}) with respect to the rarefaction parameter h when $|B|$ increases.

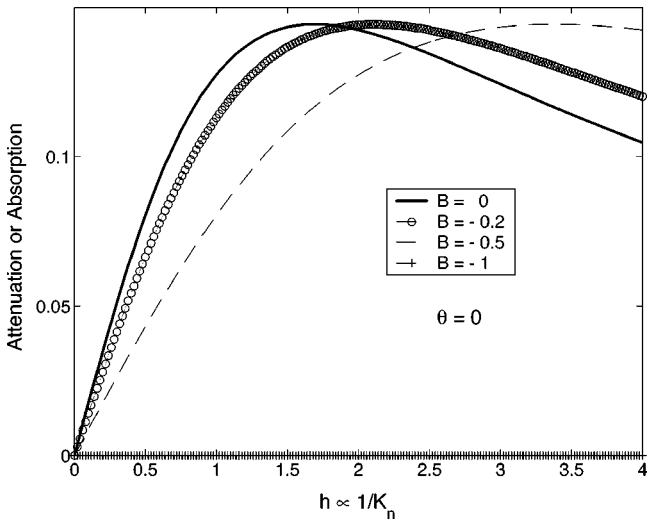

FIG. 2. Variations of the attenuation λ_i with respect to h for different B's: $\theta=0$ in different Pauli blocking parameters ($B=0$, -0.2, and -0.5, 1). There is no attenuation for $B=-1$ and all h.

To examine the detailed disorder effect, which is to introduce a free orientation θ into our approach,[7,15,16] we show some of the results for which $\theta=0$ and $\theta=0.78$ in Figs. 2 and 3. We also tune B to check the Pauli blocking effects especially when $B<0$ in these presentations. Once the free orientation or disorder θ is introduced, we observe that as the disorder (θ) increases, the dispersion value [$\lambda_r = k_r c/(\sqrt{2}\omega)$] will reach the hydrodynamical limit ($h\to\infty$)

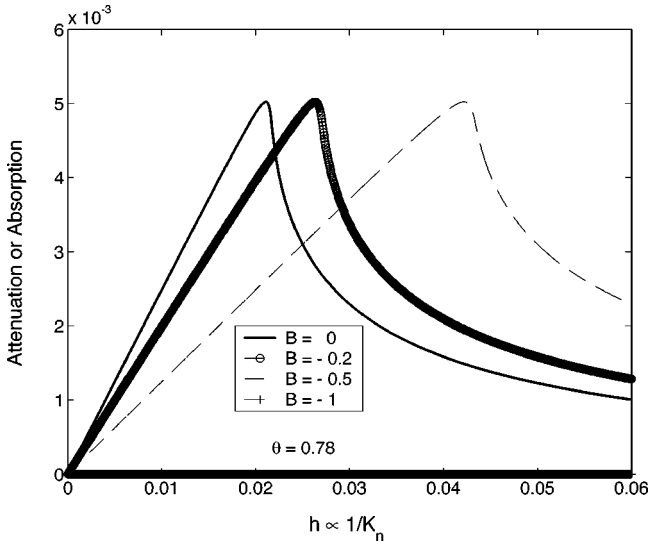

FIG. 3. Variations of the attenuation λ_i with respect to h for different B's: $\theta=0.78$ in different Pauli blocking parameters ($B=0$, -0.2, and -0.5, 1). There is no attenuation for $B=-1$ and all h.

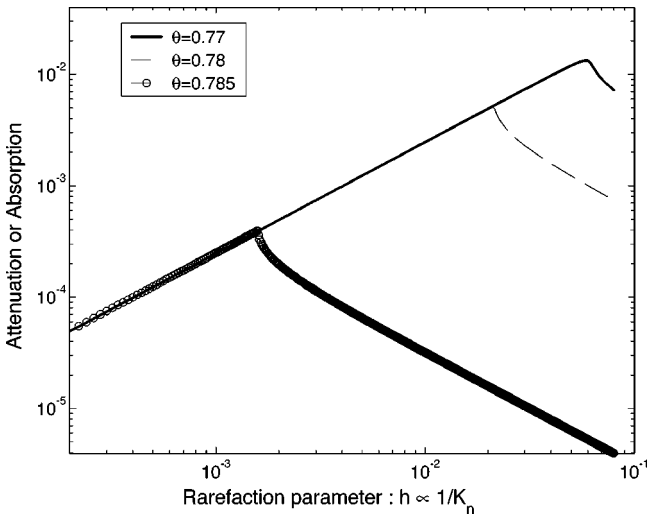

FIG. 4. Variations of the attenuation λ_i with respect to h for different disorders: $\theta=0.77$, 0.78, and 0.785 in the same Pauli blocking parameter (γ or B). h is within the rather low-density regime.

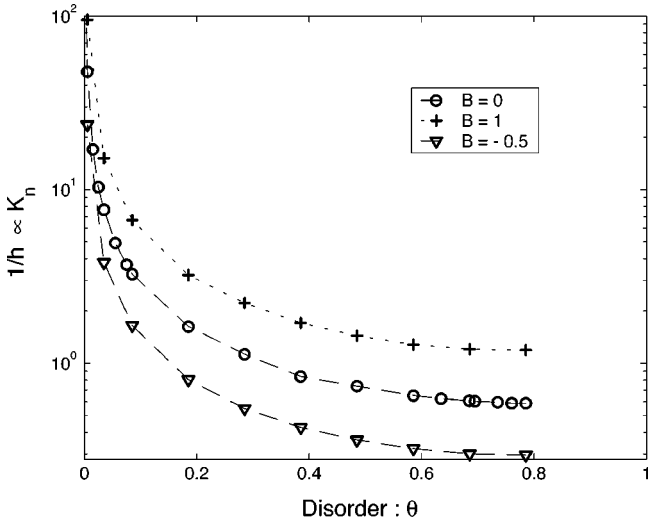

FIG. 6. Possible phase diagram for non-Fermi gases with respect to the disorder and the Knudsen number ($K_n \propto$ the mean free path).

later.[15,16] Meanwhile, the maximum absorption [or attenuation $\lambda_i=k_i c/(\sqrt{2}\omega)$] for all the rarefaction parameters h keeps decreasing as θ increases, as observed in Figs. 2 and 3 or Refs. 15 and 16. There are also shifts of the maximum absorption state (h_{max}) with respect to the rarefaction parameter h when θ increases (up to $\pi/4\sim0.7853$).

If there is no rarefaction effect ($h=0$), we have only real roots for all the models.[17] Once $h\neq0$, the imaginary part appears and the spectra diagram for each model looks entirely different. To illustrate the specific behavior of the attenuation or absorption for smaller disorder (near $\theta=\pi/4$) in the near vacuum regime ($h\gg1$), we plot three different

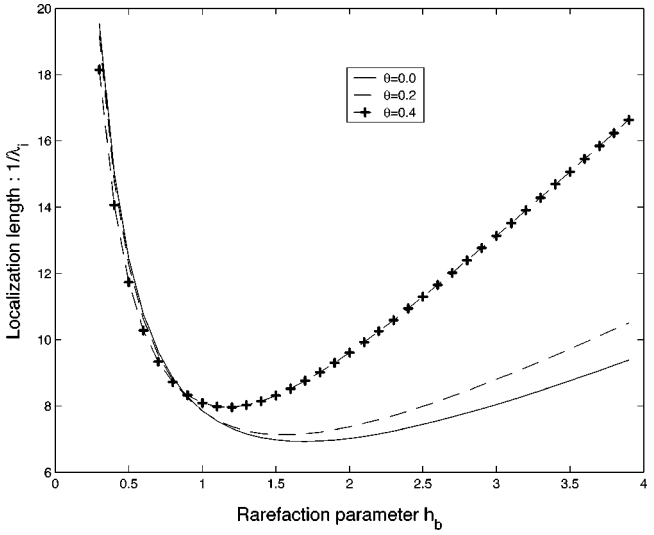

FIG. 5. Disorder (θ) effects on the localization length ($1/\lambda_i$). The energy E (relevant to the illustration of localized states in Ref. 9) corresponds to $\hbar\omega$ (Refs. 9 and 11) and $h=4cSN_0/\omega$. Thus, $E\propto1/h$ once cSN_0 is fixed. The minimum occurs around $h\sim1$ [whereas, as shown in Ref. 9, the minimum is near $Ea/c\sim0.9$; cf. Fig. 5(a) in Ref. 9] $h_b=h(1+B)$.

cases, $\theta=0.77$,0.78, and 0.785, in Fig. 4. We noticed that, as reported before,[15,16] at $\theta=\pi/4$, there is no attenuation or absorption, i.e., $\lambda_r=1.0$ and $\lambda_i=0.0$. This means the disorder or its effect is nearly zero at this (θ) value. This result also provides a good verification for the experimental side mentioned in Refs. 10–12 (acoustical analog here) as there is no loss for this particular case (θ being a disorder parameter but fixed as $\pi/4$). We also notice that around $h\sim h_{max}$, as shown in Fig. 1 or 2, there exists a trend for the absence of diffusion (λ_i starts decreasing rapidly).

Note that, for the larger (absolute value of λ) branch (the anomalous one which is similar to those propagations of diffusion modes or entropy waves reported in Refs. 15 and 16), there is a discontinuity near $\theta=0$. Once θ increases from zero, there exists a gap. Spectra (both λ_r and λ_i) will span from the far infinity and then approach to the asymptotic case $\theta=0.7853$ (near $\pi/4$) which accounts for the propagation of the diffusion mode or entropy wave. We noticed that from the definition of h_b or K_n, $h_b=f_{collision}/f_{sound}$, where f_{sound} (cf. that used in Ref. 9) is related to the classical frequency ω as discussed in the *Introduction* [cf. Eqs. (1) and (2)], so that it is relevant to the energy E as defined for the localization; thus we can estimate the localization length from those figures which vary with h_b. Based on these considerations and Eqs. (1) and (2), the relation for the possible localization length versus the frequency ($h\propto1/\omega$) extracted from our results [especially in Fig. 2; the attenuation or absorption defined here is related to the *inverse* measure of (say, one wave) length; then corresponds to the minimum localization length in Fig. 5(a) of Ref. 9] is qualitatively similar to that reported in Ref. 9. This observation could be figured out as we schematically plot the inverse of the wave absorption $1/\lambda_i$ (per unit wave length) with respect to $h=4cSN_0/\omega$. This also shows the exponential decay of the localization length near the localized region [i.e., the absence of the further diffusion or the maximum absorption (with respect to h or the inverse of the frequency ω, a correspond-

ing measure to energy E in the quantum-mechanical sense as already explained in Sec. I)]. Thus we can also obtain similar results which resemble that reported in Fig. 5(a) of Ref. 9.

People might argue that a nonzero θ would only make the system anisotropic, but not disordered. We should remind them that the derivation of the present kinetic approach was based on the binary collision of a system of dilute particles. Once the concepts of the mean free path of the gases and the center of mass coordinate system were introduced (especially when the effective, admissible collision and the microreversibility which neglects the history when particles traverse in phase space[7,14–17] were presumed) the randomness and disorder will occur although they are explained implicitly.

We demonstrate the disorder effects to the localization length in different h or $h_b = h(1+B)$ regime in Fig. 5. The relevant x-axis parameter shown in Ref. 9 is Ea/c (a is the hard-sphere diameter, and c is the wave speed). The minimum of the localization length occurs around $h \sim 1$ (cf. that of $Ea/c \sim 0.9$ in Ref. 9). This good agreement confirms our present approach. We then illustrate in Fig. 6 the possible phase diagram for non-Fermi gases considering different disorders and Knudsen numbers ($K_n \propto$ the mean free path). This result resembles that proposed by Abrahams (possible phase diagram for ''new insulator/non-Fermi liquid metal''[1]; cf. Fig. 3 therein). Note that, K_n plays the role of r_s ($\propto$ the ratio of Coulomb energy to Fermi energy as defined in Ref. 1) since the long-range dominated cases (r_s is large) correspond to our cases of h being small or K_n being large (collisionless regime or rather-low density regime where long range interactions can still exist[1,2]).

To conclude in brief, our illustrations here, i.e., the possible localized behavior of the spectra near the range of disorders $\theta = 0$ and $\theta = \pi/4$ for different Pauli blocking parameters seem to be the same as the acoustical analog (cf. Ref. 11) of the localization found elsewhere,[8–12] even though the physical length-scale parameter used here is the mean free path of the electron gases subjected to continuous collisions. We found, for sufficiently strong interactions (which would occur at low density,[1,2] say, $h \ll 1$ or $K_n \gg 1$ in our approach), a non-Fermi-liquid state of interacting electrons ($\gamma \neq -1$ in our formulation) is stable in the presence of disorder. There will be no dissipations or attenuations (cf absence of localization[9,11,12,15–17]) once $B = -1$ or $\theta = \pi/4$ which corresponds to any h or K_n. We shall investigate more complicated problems in the future.[18–22]

ACKNOWLEDGMENT

The author was partially supported by the National Natural Science Foundation of China (NSFC) under Grant No. 10274061.

*Address after June 2004: P.O. Box 30-15, Shanghai 200030, PR China.

[1] E. Abrahams, Ann. Phys. (Leipzig) **8**, 539 (1999).
[2] E. Abrahams, S.V. Kravchenko, and M.P. Sarachik, Rev. Mod. Phys. **73**, 251 (2001).
[3] N.F. Mott, Rep. Prog. Phys. **47**, 909 (1984); R.J. Bell, *ibid.* **35**, 1315 (1972). P.W. Anderson, Comments Solid State Phys. **2**, 193 (1970).
[4] A.P. Taylor and A. MacKinnon, J. Phys.: Condens. Matter **14**, 8663 (2002); V. Dobrosavljević *et al.*, Phys. Rev. Lett. **79**, 455 (1997).
[5] A.J. Leggett, Rev. Mod. Phys. **73**, 307 (2001); F. Dalfovo, S. Giorgini, L.P. Pitaevskii, and S. Stringari, *ibid.* **71**, 463 (1999).
[6] H.O. Kneser, in *Handbuch der Physik*, edited by S. Flügge (Bd. XI/1, Springer, Berlin, 1961), p. 129; H. Grad, SIAM (Soc. Ind. Appl. Math.) J. Appl. Math. **14**, 932 (1966); L. Sirovich, J. Math. Phys. **10**, 239 (1969).
[7] A.K.-H. Chu, J. Phys. B **34**, L711 (2001).
[8] S. John, Phys. Today **44**, 32 (1991); A. Klein and A. Koines, Math. Phys. Anal. Geom. **4**, 97 (2001); M. Aizenman, J.H. Schenker, R.M. Friedrich, and D. Hundertmark, Commun. Math. Phys. **224**, 219 (2001).
[9] T.R. Kirkpatrick, Phys. Rev. B **31**, 5746 (1985).
[10] A. Figotin, J. Stat. Phys. **73**, 571 (1993); A. Ishimaru, *Wave Propagation and Scattering in a Random Media* (Academic Press, New York, 1978); G. François and A. Klein, Commun. Math. Phys. **222**, 415 (2001); P. Sheng, *Introduction to Wave Scattering, Localization, and Mesoscopic Phenomena* (Academic Press, New York, 1995).
[11] J.D. Maynard, Rev. Mod. Phys. **73**, 401 (2001).
[12] P.W. Anderson, Phys. Rev. **109**, 1492 (1958); A. Figotin and A. Klein, Commun. Math. Phys. **180**, 439 (1996).
[13] V.V. Vedenyapin, I.V. Mingalev, and O.V. Mingalev, Russian Academy of Sciences Sbornik Mathematics **80**, 271 (1995); E. Giglio, E. Suraud, and P.-G. Reinhard, Ann. Phys. (Leipzig) **11**, 291 (2002).
[14] T. Platkowski and R. Illner, SIAM Rev. **30**, 213 (1988); N. Bellomo and T. Gustafsson, Rev. Math. Phys. **3**, 137 (1991).
[15] K.-H.W. Chu, J. Phys. A **35**, 1919 (2002).
[16] A.K.-H. Chu, Phys. Rev. E **66**, 047106 (2002); W.K.-H. Chu, Appl. Math. Lett. **14**, 275 (2001).
[17] A.K.-H. Chu (unpublished).
[18] M.I. Stockman, S.V. Faleev, and D.J. Bergman, Phys. Rev. Lett. **87**, 167401 (2001); L.L. Foldy, Phys. Rev. **67**, 107 (1945); M. Lax, Rev. Mod. Phys. **23**, 287 (1951).
[19] C.A. Condat and T.R. Kirkpatrick, Phys. Rev. B **36**, 6782 (1987); G. Blatter, V.B. Geshkenbein, and N.B. Kopnin, *ibid.* **59**, 14 663 (1999); G. Modugno *et al.*, Science **297**, 2240 (2002).
[20] M. Notomi *et al.*, Phys. Rev. Lett. **87**, 253902 (2001); L.A. Bunimovich and M.A. Khlabystova, J. Stat. Phys. **104**, 1155 (2001); L. Banyai and P. Gartner, Phys. Rev. Lett. **88**, 210404 (2002).
[21] D. Damanik and P. Stollmann, Geom. Funct. Anal. **11**, 11 (2001); E. Braaten *et al.*, Phys. Rev. Lett. **88**, 040401 (2002).
[22] R. Resta, J. Phys.: Condens. Matter **14**, R625 (2002); Yu.V. Tarasov, *ibid.* **14**, L357 (2002); O. Halfpap, Ann. Phys. (Leipzig) **10**, 623 (2001).